IOPscience iopscience.iop.org

Home Search Collections Journals About Contact us My IOPscience

Theoretical study of density-dependent intraexcitonic transitions in optically excited quantum wells

This content has been downloaded from IOPscience. Please scroll down to see the full text.

2011 J. Phys.: Condens. Matter 23 345801

(http://iopscience.iop.org/0953-8984/23/34/345801)

View the table of contents for this issue, or go to the journal homepage for more

Download details:

IP Address: 202.117.17.90
This content was downloaded on 18/12/2016 at 05:21

Please note that terms and conditions apply.

You may also be interested in:

Quantum states and optical responses of low-dimensional electron–hole systems
Tetsuo Ogawa

The dynamic Stark effect under a not-too-strong femtosecond excitation regime in quantum well structures
Sharmila Banerjee, Pratima Sen and Pranay K Sen

Femtosecond spectroscopy in semiconductors
V M Axt and T Kuhn

Pair-excitation energetics of highly correlated many-body states
M Mootz, M Kira and S W Koch

Mott transition of excitons in GaAs-GaAlAs quantum wells
G Manzke, D Semkat and H Stolz

Spin dynamics of low-dimensional excitons due to acoustic phonons
A Thilagam and M A Lohe

Stark effect of interactive electron–hole pairs in spherical semiconductor quantumdots
B Billaud, M Picco and T-T Truong

Models of coherent exciton condensation
P B Littlewood, P R Eastham, J M J Keeling et al.

Experimental methods and analysis of cold and dense dipolar exciton fluids
Ronen Rapaport and Gang Chen

IOP PUBLISHING JOURNAL OF PHYSICS: CONDENSED MATTER
J. Phys.: Condens. Matter **23** (2011) 345801 (9pp) doi:10.1088/0953-8984/23/34/345801

Theoretical study of density-dependent intraexcitonic transitions in optically excited quantum wells

Dawei Wang, Xiaoli Lei and Zhaoxin Wu

Key Laboratory for Physical Electronics and Devices of the Ministry of Education, School of Electronic and Information Engineering, Xi'an Jiaotong University, Xi'an 710049, People's Republic of China

E-mail: dawei.wang@mail.xjtu.edu.cn

Received 11 February 2011, in final form 20 June 2011
Published 12 August 2011
Online at stacks.iop.org/JPhysCM/23/345801

Abstract

We present a theoretical study of the terahertz-pulse-induced intraexcitonic dynamics of optically created excitons in quantum wells, providing an explanation of the density dependence of the 1s–2p intraexcitonic transitions observed experimentally. We find that two types of many-body interactions, the phase space filling and the exchange interaction, are responsible for the observed red-shift of the resonance frequency. In addition to calculating the density renormalized exciton energy levels, which offer indirect information regarding the density-dependent 1s–2p transitions, we developed a mean-field approach to examine the intraexcitonic transition process directly. The resulting dynamic equation provides a useful tool to gain insight into the intraexcitonic transitions in semiconductor nanostructures.

(Some figures in this article are in colour only in the electronic version)

1. Introduction

Accompanying the development of terahertz (THz) technology over the years, transient THz spectroscopy has become an important experimental technique to understand low energy resonances in various systems. Initially, this technique was used to monitor the lifetime or population of ground state excitons [1, 2] or observe far infrared (FIR) absorption by magnetoexcitons [3, 4]. In recent years, it has also been used to understand the quantum state of the ground state exciton itself, and the dynamics related to many-body interactions involved [5, 6]. The density influence on intraexcitonic transitions was a less explored topic until recently when THz spectroscopy became a standard technique [7, 8]. The transitions between internal excitonic states have been investigated in many systems such as Cu_2O [5, 9–13], GaAs/AlGaAs quantum wells [2, 6, 7, 14–16], and superlattices [8] by many research groups, employing FIR or THz spectroscopy [1, 2, 5–7, 9–16]. The optical-pump-THz-probe study of the intraexcitonic 1s–2p transition in GaAs/$Al_xGa_{1-x}As$ quantum wells [7] clearly demonstrate that this process is strongly density dependent, with the resonance frequency of the 1s–2p transition decreasing with increasing exciton densities. Additional experiments were performed thereafter using similar techniques [12, 15, 17], and the excitonic contribution to the THz dielectric response is theoretically obtained using Fermi's golden rule [15].

Theoretical investigations of the density influence on exciton internal states, notably by Schmitt-Rink *et al* [19], focused on the 1s exciton state in quantum well structures and successfully explained the observed blue-shift of the 1s excitonic state in experiments [18, 20]. In this paper, we will present a general method, which includes many-body interactions between excitons [21, 22], to investigate the density influence on exciton energy levels and the intraexcitonic dynamics of optically excited excitons in quantum wells. Our aim is not to compete with other advanced theories like the comprehensive theory proposed by Kira *et al* [23]. Instead, we want to provide a straightforward method that can be readily used to understand and estimate how exciton densities can influence the intraexcitonic transitions and, in particular, the resonance shift associated with these transitions.

 © 2011 IOP Publishing Ltd Printed in the UK & the USA

Optically excited excitons, unlike an atomic system, have special properties because they are composite particles and are not true bosons. Thus, one has to be careful to include the essential many-body interactions in an excitonic system to investigate its dynamics and at the same time keep the arising theoretical problem tractable. It has been shown in a previous work [21] that, to the Hartree–Fock order, there are two such interactions that correlate excitons: the phase space filling (PSF) effect and the exchange interaction. The influence of these two effects on the interband excitonic dynamics was investigated using the density matrix method [21, 22]. However, their influence on the THz-pulse-induced intraexcitonic transitions is still unclear. Employing a quasi-boson approach (compare with section 2), there are two ways to investigate the intraexcitonic dynamics in a semiconductor nanostructure. In section 3.1, we will find how each exciton internal state is affected by exciton densities, thus obtaining the intraexcitonic transition frequencies indirectly. A second method, which will be shown in section 3.2, deals with the intraexcitonic dynamics directly. In this method, we first construct a mean-field wavefunction for a system of excitons resonantly excited to the 1s excitonic state and then we compute the deviation from this mean-field wavefunction caused by a THz pulse using a variational approach. The resulting dynamic equation for the deviation is used to describe the THz-pulse-induced intraexcitonic transitions. Finally, we use the derived equation to study the 1s–2p intraexcitonic transition directly and connect the observed red-shift to many-body interactions.

This paper is organized as follows. In section 2, we briefly introduce the quasi-boson Hamiltonian, the quasi-boson dynamic equation, and summarize our excitonic approach [21, 22]. In section 3, we present two theoretical methods to investigate the density dependence of the intraexcitonic transitions between 1s and 2p exciton states, and then discuss the applicability of the adopted theoretical methods. Finally, in section 4, we present our conclusions.

2. The quasi-boson approach

In an excitonic approach, excitons are viewed as fundamental excitations of optically excited semiconductors or semiconductor nanostructures. One distinct feature of an excitonic approach is that it can treat the intraband dynamics as transitions between two internal excitonic states [24]. In this approach, the PSF effects associated with the composite nature of excitons need to be treated with care [25, 26]. One common practice is to assume a low exciton density so that PSF effects are negligible [24, 27, 28]. However, to understand the density dependence of intraexcitonic transitions, we need to use the density-independent quasi-bosonic exciton creation and annihilation operators, and explicitly take into account their density-dependent commutation relations [21, 24, 29, 30]. As we will investigate the dynamics of excitons and the density influence on the resonance of intraexcitonic transitions, we focus on the picosecond time scale (∼1 ps) in which most bound excitons are in the $\mathbf{K} = 0$ center of mass (COM) momentum state. This makes possible the use of our approach that includes only $\mathbf{K} = 0$ excitons.

One way to describe the wavefunction of an exciton is to use its Fourier coefficients. This method, when further developed, requires us to introduce the quasi-boson operator $B^\dagger_{\mathbf{q}}$, which is closely related to the true exciton creation operator $B^\dagger_\mu$ (details about $B^\dagger_{\mathbf{q}}$ and $B^\dagger_\mu$ will be shown below). The resulting dynamic equation for $B^\dagger_{\mathbf{q}}$ is crucial in determining the density influence on excitonic energy levels, and it will be our starting point for constructing a mean-field theory to directly examine intraexcitonic transitions in section 3.2.

The quasi-boson creation operator, $B^\dagger_{\mathbf{k}}$, which represents the creation of an electron–hole pair, is defined as [21]

$$B^\dagger_{\mathbf{k}} = OU(\alpha^\dagger_{\mathbf{k}}\beta^\dagger_{-\mathbf{k}})U^\dagger O^\dagger, \tag{1}$$

where $\alpha^\dagger_{\mathbf{k}}$ ($\beta^\dagger_{-\mathbf{k}}$) is the electron (hole) creation operator, here $\mathbf{k}$ is the momentum of the electron in the electron–hole pair. The Usui transformation U [31] and the ordering operator O are necessary to map fermion operators to the quasi-boson operator [21, 32], $B^\dagger_{\mathbf{k}}$. The true exciton creation operator is obtained with a canonical transformation

$$B^\dagger_\mu = \sum_{\mathbf{k}} c^{\mathbf{k}}_\mu B^\dagger_{\mathbf{k}}, \tag{2}$$

where μ denotes the internal state of an exciton and $c^{\mathbf{k}}_\mu$ is the expansion coefficient that can be obtained from exciton wavefunctions. Since $B^\dagger_{\mathbf{k}}$ represents quasi-bosons, it has a special commutation relation [21],

$$[B_{\mathbf{k}}, B^\dagger_{\mathbf{k}'}] = \delta_{\mathbf{k},\mathbf{k}'}(1 - 2B^\dagger_{\mathbf{k}}B_{\mathbf{k}}), \tag{3}$$

and a supplementary condition

$$B^\dagger_{\mathbf{k}}B^\dagger_{\mathbf{k}} = 0. \tag{4}$$

Using the Usui transformation, we can transform the Hamiltonian of a photoexcited semiconductor system [33] in fermion space to obtain the Hamiltonian H in the quasi-boson pair space. The details of the transformation process can be found in [29], we thus only present the results here. The Hamiltonian in the quasi-boson basis can be written as

$$H = H_X + H_C + H_I. \tag{5}$$

In equation (5),

$$H_X = \sum_{\mathbf{k}} E^0_{\mathbf{k}} B^\dagger_{\mathbf{k}} B_{\mathbf{k}} - \sum_{\mathbf{k}_1,\mathbf{k}_2} V_{\mathbf{k}_1-\mathbf{k}_2} B^\dagger_{\mathbf{k}_2} B_{\mathbf{k}_1} \tag{6}$$

is the Hamiltonian for non-interacting quasi-boson pairs where the Coulomb interaction inside the pair is included as the second term.

$$H_C = -\sum_{\mathbf{k}_1,\mathbf{k}_2} V_{\mathbf{k}_1-\mathbf{k}_2} B^\dagger_{\mathbf{k}_1} B^\dagger_{\mathbf{k}_2} B_{\mathbf{k}_2} B_{\mathbf{k}_1} \tag{7}$$

describes the exchange interaction and

$$H_I = -\sum_{\mathbf{k}} \boldsymbol{\mathcal{E}}(t) \cdot (\mathbf{d}_{cv} B^\dagger_{\mathbf{k}} + \text{h.c.}) \tag{8}$$

describes the interaction of quasi-boson pairs with the laser electric field, $\boldsymbol{\mathcal{E}}(t)$.

The commutation relation, equation (3), is used to develop the dynamic equation for $B^{\dagger}_{\mathbf{k}}$, which is given by

$$\begin{aligned}\mathrm{i}\hbar\frac{\mathrm{d}}{\mathrm{d}t}B^{\dagger}_{\mathbf{p}} &= -\sum_{\mathbf{k}}[(E_{\mathrm{g}}+V_0+\epsilon^{\mathrm{e}}_{\mathbf{p}}+\epsilon^{\mathrm{h}}_{-\mathbf{p}})\delta_{\mathbf{k},\mathbf{p}}-V_{\mathbf{p}-\mathbf{k}}]B^{\dagger}_{\mathbf{k}}\\ &\quad+2\sum_{\mathbf{k}}V_{\mathbf{p}-\mathbf{k}}B^{\dagger}_{\mathbf{p}}B^{\dagger}_{\mathbf{k}}B_{\mathbf{k}}-2\sum_{\mathbf{k}}V_{\mathbf{p}-\mathbf{k}}B^{\dagger}_{\mathbf{k}}B^{\dagger}_{\mathbf{p}}B_{\mathbf{p}}\\ &\quad+\boldsymbol{\mathcal{E}}(t)\cdot\mathbf{M}_{cv}-2\boldsymbol{\mathcal{E}}(t)\cdot\mathbf{M}_{cv}B^{\dagger}_{\mathbf{p}}B_{\mathbf{p}}\\ &\quad+E_{\mathrm{THz}}(t)\sum_{\mathbf{q}}K_{\mathbf{q},\mathbf{p}}B^{\dagger}_{\mathbf{q}}(1-2B^{\dagger}_{\mathbf{p}}B_{\mathbf{p}}),\end{aligned}\tag{9}$$

where E_{g} is the energy gap between the valence band and the conduction band, $\epsilon^{\mathrm{e}}_{\mathbf{p}}$ ($\epsilon^{\mathrm{h}}_{-\mathbf{p}}$) is the kinetic energy of an electron (hole), $V_{\mathbf{q}}$ is the Coulomb interaction matrix in the momentum space, $\mathbf{M}_{cv}$ is the interband transition matrix, and $K_{\mathbf{p},\mathbf{q}}$ is the transition matrix between quasi-boson states, which can be computed from exciton wavefunctions [24]. There are two external pulses: the optical pulse $\boldsymbol{\mathcal{E}}(t)$ and the THz pulse $E_{\mathrm{THz}}(t)$ that follows the optical one.

Using the dynamic equation (9) and the canonical transformation (2) we can derive a dynamic equation for true exciton creation operators $B^{\dagger}_{\mu}$:

$$\begin{aligned}&\mathrm{i}\hbar\frac{\mathrm{d}}{\mathrm{d}t}\langle B^{\dagger}_{\mu}\rangle+E_{\mu}\langle B^{\dagger}_{\mu}\rangle\\ &\quad=-\mathrm{i}\hbar\frac{\langle B^{\dagger}_{\mu}\rangle}{T^{\mathrm{EXE}}_{\mathrm{inter}}}+2\sum_{\mu_1,\mu_2,\mu_3}R^{\mu}_{\mu_1,\mu_2,\mu_3}\langle B^{\dagger}_{\mu_1}\rangle\langle B^{\dagger}_{\mu_2}B_{\mu_3}\rangle\\ &\quad\quad+\boldsymbol{\mathcal{E}}(t)\cdot\mathbf{M}^{*}_{cv}\left(C_{\mu}-2\sum_{\mu_1,\mu_2}C_{\mu,\mu_1,\mu_2}\langle B^{\dagger}_{\mu_1}B_{\mu_2}\rangle\right),\end{aligned}\tag{10}$$

where

$$R^{\mu}_{\mu_1,\mu_2,\mu_3}=R1^{\mu}_{\mu_1,\mu_2,\mu_3}-R2^{\mu}_{\mu_1,\mu_2,\mu_3},\tag{11}$$

$$R1^{\mu}_{\mu_1,\mu_2,\mu_3}=\sum_{\mathbf{k},\mathbf{p}}V_{\mathbf{p}-\mathbf{k}}c^{\mathbf{p}}_{\mu}c^{\mathbf{p}*}_{\mu_1}c^{\mathbf{k}*}_{\mu_2}c^{\mathbf{k}}_{\mu_3},\tag{12}$$

$$R2^{\mu}_{\mu_1,\mu_2,\mu_3}=\sum_{\mathbf{k},\mathbf{p}}V_{\mathbf{p}-\mathbf{k}}c^{\mathbf{p}}_{\mu}c^{\mathbf{p}*}_{\mu_2}c^{\mathbf{k}*}_{\mu_1}c^{\mathbf{p}}_{\mu_3},\tag{13}$$

$$C_{\mu}=\sum_{\mathbf{p}}c^{\mathbf{p}}_{\mu},\tag{14}$$

$$C_{\mu,\mu_1,\mu_2}=\sum_{\mathbf{p}}c^{\mathbf{p}}_{\mu}c^{\mathbf{p}*}_{\mu_1}c^{\mathbf{p}}_{\mu_2},\tag{15}$$

E_{μ} is the energy of an exciton with internal state μ, and $T^{\mathrm{EXE}}_{\mathrm{inter}}$ is the phenomenological interband dephasing time constant (we have removed the THz term in equation (9) for simplicity). This dynamic equation had been used to study the ultrafast optical response of one-dimensional (1D) and two-dimensional (2D) semiconductor nanostructures [21, 22] via the density matrix method. The coefficients defined in equations (11)–(15) have shown their importance in analyzing the blue-shift and bleaching of 1s exciton resonance [22].

3. Density-dependent intraexcitonic transitions

After introducing the quasi-boson approach, we now use it to investigate the density-dependent intraexcitonic transitions that have attracted much interest in recent years [7, 12, 15]. It was experimentally found that the resonance frequency of the 1s–2p transition is strongly dependent on exciton densities [7] and that the resonance frequency is red-shifted as exciton density increases. It is worth noting that the magnitude of this red-shift is about four times larger than that of the blue-shift of 1s excitons [18, 19]. To fully understand the cause of this large red-shift theoretically, we use two different methods in sections 3.1 and 3.2. First, we calculate the density dependence of individual exciton states, and find the energy difference between the 1s and 2p states. This method is similar to that shown in [19], but is more systematic in that it can be applied to an arbitrary exciton state. Second, we will develop a mean-field theory to directly examine the intraexcitonic process. This will provide a foundation for using the renormalized exciton energy levels to evaluate the resonance frequency of intraexcitonic transitions.

3.1. Density influence on exciton energy levels

Rearranging equation (10), we have

$$\begin{aligned}&\mathrm{i}\hbar\frac{\mathrm{d}}{\mathrm{d}t}\langle B^{\dagger}_{\mu}\rangle+\left(E_{\mu}-2\sum_{\mu_2,\mu_3}R^{\mu}_{\mu,\mu_2,\mu_3}\langle B^{\dagger}_{\mu_2}B_{\mu_3}\rangle\right)\langle B^{\dagger}_{\mu}\rangle\\ &\quad=-\mathrm{i}\hbar\frac{\langle B^{\dagger}_{\mu}\rangle}{T^{\mathrm{EXE}}_{\mathrm{inter}}}+2\sum_{\mu_1\neq\mu,\mu_2,\mu_3}R^{\mu}_{\mu_1,\mu_2,\mu_3}\langle B^{\dagger}_{\mu_1}\rangle\langle B^{\dagger}_{\mu_2}B_{\mu_3}\rangle\\ &\quad\quad+\boldsymbol{\mathcal{E}}(t)\cdot\mathbf{M}^{*}_{cv}\left(C_{\mu}-2\sum_{\mu_1,\mu_2}C_{\mu,\mu_1,\mu_2}\langle B^{\dagger}_{\mu_1}B_{\mu_2}\rangle\right),\end{aligned}\tag{16}$$

which indicates that the excitonic energy level E_{μ} changes with the number of excitons in the system according to the following equation:

$$\delta E_{\mu}=-2\sum_{\mu_2,\mu_3}R^{\mu}_{\mu,\mu_2,\mu_3}\langle B^{\dagger}_{\mu_2}B_{\mu_3}\rangle,\tag{17}$$

which can be readily applied to different exciton energy levels. When 1s excitons dominate the system (which is the case when 1s excitons are resonantly excited), the change to the 1s exciton state caused by interactions between excitons is given by

$$\delta E_{1\mathrm{s}}\simeq-2R^{1\mathrm{s}}_{1\mathrm{s},1\mathrm{s},1\mathrm{s}}\langle B^{\dagger}_{1\mathrm{s}}B_{1\mathrm{s}}\rangle,\tag{18}$$

where $R^{1\mathrm{s}}_{1\mathrm{s},1\mathrm{s},1\mathrm{s}}$ can be analytically obtained for a strict 2D system, and numerically for a general quantum well structure [32]. For a strict 2D system, we have

$$\begin{aligned}\delta E_{1\mathrm{s}}&\simeq 32\pi a^2_{2\mathrm{D}}\left(1-\frac{315\pi^2}{2^{12}}\right)E_{1\mathrm{s}}n_{1\mathrm{s}}\\ &=24.2E_{\mathrm{b}}a^2_{2\mathrm{D}}n_{1\mathrm{s}},\end{aligned}\tag{19}$$

where $n_{1\mathrm{s}}$ is the areal density of 1s excitons, E_{b} is the binding energy of a 1s exciton, and $a_{2\mathrm{D}}$ is the radius of a 2D 1s

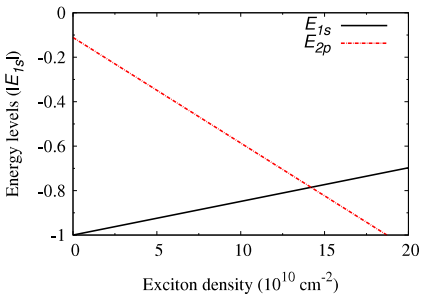

Figure 1. Variation of the 1s and 2p excitonic energy levels, in units of $|E_{1s}|$, in a strictly 2D system with the areal 1s exciton density.

exciton [19]. Similarly, for the 2p exciton state, we have

$$\delta E_{2p} \simeq -2R^{2p}_{2p,1s,1s}\langle B^{\dagger}_{1s}B_{1s}\rangle, \\ = -76.0E_b a^2_{2D} n_{1s}. \quad (20)$$

It is interesting to note that, while the energy of the 1s exciton state increases with exciton density [18, 19], that of the 2p state decreases. This difference between 1s and 2p excitonic states shows that the delicate balance between the PSF and exchange interactions can result in different behavior for different excitonic states. Figure 1 shows the energy levels of 1s and 2p states as a function of 1s exciton density (the parameter $a_{2D} = 25$ Å)[1]. The linear increase of E_{1s} (blue-shift) has already been reported [18, 19], but the behavior of the 2p exciton state was unclear for two reasons. First, unlike 1s excitons, 2p excitons cannot be directly excited by an optical pulse; second, theoretical analysis becomes more difficult than the 1s exciton state using the method presented in [19].

As we can see, equation (17) provides a systematic method for estimating the density dependence of exciton energy levels. It can be applied to an arbitrary exciton state, and can include the effects due to different exciton states (e.g. n_{1s}, n_{2s} ...) when it is desired. The basic procedure for obtaining δE_μ is as follows: (1) find exciton wavefunctions in the system [34–36]; (2) obtain the coefficients $c^{\mathbf{p}}_\mu$ from exciton wavefunctions [22]; (3) find δE_μ by calculating relevant $R^\mu_{\mu_1,\mu_2,\mu_3}$s [32]. As another example, we investigate how the resonance of 2s excitons is affected by 1s exciton densities. Assuming 1s excitons are resonantly excited and dominate the system, the energy shift of 2s excitons is given by

$$\delta E_{2s} \simeq -2R^{2s}_{1s,1s,1s}\langle B^{\dagger}_{1s}B_{1s}\rangle. \quad (21)$$

After obtaining $R^{2s}_{2s,1s,1s}$ numerically (for a strictly 2D system), we have

$$\delta E_{2s} = -85.4E_b a^2_{2D} n_{1s}, \quad (22)$$

which clearly shows that the resonance of 2s excitons is red-shifted, in contrast to the result for 1s excitons (compare with equation (19)), and is in line with the experimental observation that 2s excitonic resonance is consistently red-shifted for increased exciton density under resonant excitation conditions (the pumping pulse is resonant with the 1s excitonic state) [37]. The red-shift of the resonance is mainly determined by the fact that, in the case of the 2s excitonic state, the PSF is overwhelmed by the exchange interaction in the system, giving rise to different results for 1s, 2s, and 2p states.

We note that several factors can cause some difference between our theoretical prediction and experimental results. First, different excitation conditions can result in different δE_{1s} and δE_{2p}. Since the dynamic equation (equation (10)) does not include electron spin, we essentially model a system excited by a circularly polarized laser pulse. If a linearly polarized laser pulse is used, we should have $\delta E_{1s} \simeq 12.1E_b a^2_{2D} n_{1s}$ and $\delta E_{2p} \simeq -38.0E_b a^2_{2D} n_{1s}$, where a factor of 0.5 has arisen when electron spins are considered [19, 32] (note that $\delta E_{1s}/\delta E_{2p}$ does not change). Second, we need to have a proper estimation of a_{2D}, which is often hard to obtain in experiments, to use the results in equations (19) and (20). Finally, to have a quantitative comparison with experiments, we need to work with real quantum wells [32], for which no analytical expression can be obtained. It is generally expected that the energy shifts due to many-body interactions are weaker in real quantum wells than in a strictly 2D system.

Obtaining the density dependence of individual exciton energy levels is not the end of our investigation because there are two remaining problems: (1) unlike the 1s state, the 2p state cannot be directly excited by an optical pulse (in equation (16), $C_{2p} = 0$). Thus the use of $\delta E_{2p} = -2\sum_{\mu_2,\mu_3} R^{2p}_{2p,\mu_2,\mu_3}\langle B^{\dagger}_{\mu_2}B_{\mu_3}\rangle$, which is derived from equation (16), is not as intuitively compelling as the result for the 1s exciton state, its interpretation and value can easily be questioned. (2) According to Fermi's golden rule, the resonance of the THz-pulse-induced 1s to 2p intraexcitonic transition would have

$$\hbar\omega_{1s-2p} = E_{1s} - E_{2p}, \quad (23)$$

and will give the correct result if only one exciton exists in the system. However, it is unclear if equation (23) is still valid when many-body interactions are included and the dependences of E_{1s} and E_{2p} on exciton density are considered. To address these concerns, the THz-pulse-induced intraexcitonic transition process will be examined using a mean-field method in section 3.2.

3.2. Mean-field method for THz-pulse-induced intraexcitonic transitions

In this section, we further examine the THz-pulse-induced intraexcitonic transitions directly using a mean-field method. Starting from equation (9), we will construct an effective action that employs the wavefunction $\psi_{\mathbf{k}}(t)$, which transcribes the dynamics of the operator $B^{\dagger}_{\mathbf{k}}$ into a complex number (we will specify the properties of $\psi_{\mathbf{k}}$ below). This method has several advantages. First, it demonstrates that the exciton system can be described by an ensemble of two-level systems distributed at different $\mathbf{k}$ points (compare with figure 2), and that these two-level systems can interact with each other.

[1] We note that $a_{2D} = a_0/4$, where a_0 is the Bohr radius of a 1s exciton in bulk semiconductors (compare with [19]).

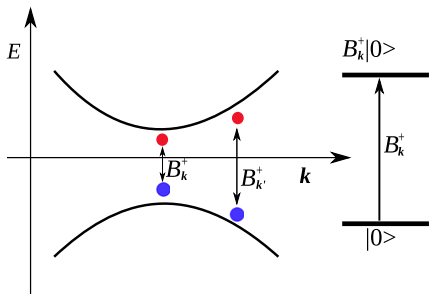

Figure 2. In an optically excited quantum well, electron–hole pairs are created at different **k**s. At each **k**, the quantum state is given by a superposition of the vacuum state $|0_{\mathbf{k}}\rangle$ and the excited state $B_{\mathbf{k}}^{\dagger}|0_{\mathbf{k}}\rangle$.

Second, in this method the phase associated with $\psi_{\mathbf{k}}$ can be conveniently treated (like a real two-level system, this phase turns out to be important). Finally, by constructing an effective action, many theoretical techniques, such as the variational method, the Green's function method, and the linear response theory can be explored to study different experimental situations.

The basic properties of $\psi_{\mathbf{k}}$ can be inferred from the properties of $B_{\mathbf{k}}^{\dagger}$. The commutation relation in equation (3) and the condition in equation (4) strongly suggest that $B_{\mathbf{k}}^{\dagger}$ is the raising operator of a two-level system at **k**. In fact, $B_{\mathbf{k}}^{\dagger}$ can be mapped onto Pauli matrices using the equivalence relations $B_{\mathbf{k}}^{\dagger} \longleftrightarrow \sigma_+^{\mathbf{k}}/2 = (\sigma_x^{\mathbf{k}} + \mathrm{i}\sigma_y^{\mathbf{k}})/2$, $B_{\mathbf{k}} \longleftrightarrow \sigma_-^{\mathbf{k}}/2 = (\sigma_x^{\mathbf{k}} - \mathrm{i}\sigma_y^{\mathbf{k}})/2$. We note that, for $\mathbf{k} \neq \mathbf{k}'$, the Pauli matrices obey the relation $[\sigma_i^{\mathbf{k}}, \sigma_j^{\mathbf{k}'}] = 0$, here $i, j = x, y, z$. After identifying $B_{\mathbf{k}}^{\dagger}$ with $\sigma_+^{\mathbf{k}}$, the excitonic Hamiltonian $H = H_X + H_C + H_I$ shown in [21] can be rewritten using Pauli matrices. The mapping of $B_{\mathbf{k}}^{\dagger}$ to $\sigma_+^{\mathbf{k}}$ and the construction of the Hamiltonian using $\sigma^{\mathbf{k}}$ indicate that an optically excited quantum well can be described by a series of $\psi_{\mathbf{k}}$ at each **k** that describes the quantum state of the electron–hole pair at **k**, i.e. the wavefunction of the system is given by

$$|\Psi\rangle = \frac{1}{\sqrt{\mathcal{N}}} \prod_{\mathbf{k}} (1 + \psi_{\mathbf{k}}^* B_{\mathbf{k}}^{\dagger})|0\rangle, \tag{24}$$

where $\mathcal{N}$ is a normalization coefficient and $|0\rangle$ denotes the vacuum state. As we can see, the quantum state at each **k** is a superposition of two levels $|0\rangle$ and $B_{\mathbf{k}}^{\dagger}|0\rangle$, with $\psi_{\mathbf{k}}^*$ being a coefficient. We note that $\psi_{\mathbf{k}}$ is the wavefunction and is also an order parameter because its values at different **k** disclose information about the coherence of the system, it is similar to the Bardeen–Cooper–Schrieffer (BCS) form for the exciton condensate wavefunction [38], and it has already been pointed out that a coherently excited semiconductor nanostructure can indeed be described by equation (24) in the mean-field sense (i.e. $\psi_{\mathbf{k}}$ being the mean field) [39, 40]. Since we are dealing with a two-level system at each **k** point, a formal expression for the mean field $|\Psi_{\mathrm{MF}}\rangle$ is given by [40]

$$|\Psi_{\mathrm{MF}}\rangle = \prod_{\mathbf{k}} (\cos\theta_{\mathbf{k}} + \mathrm{e}^{\mathrm{i}\gamma_{\mathbf{k}}} \sin\theta_{\mathbf{k}} B_{\mathbf{k}}^{\dagger})|0\rangle, \tag{25}$$

which can be reduced to equation (24). Thus $\psi_{\mathbf{k}}$ must be a complex number, and the connection between $B_{\mathbf{k}}^{\dagger}(t)$ (in the Heisenberg picture) and $\psi_{\mathbf{k}}(t)$ is shown in the following equation:

$$\langle 0|B_{\mathbf{k}}^{\dagger}(t)|0\rangle = \langle \Psi_{\mathrm{MF}}|B_{\mathbf{k}}^{\dagger}|\Psi_{\mathrm{MF}}\rangle = \psi_{\mathbf{k}}(t). \tag{26}$$

A similar procedure shows that $B_{\mathbf{k}}$ can be transcribed to $\psi_{\mathbf{k}}^*$.

We now construct an effective action from equation (9). The effective action has three parts, $S = S_0 + S_I + S_T$. S_0 is the effective action that includes the PSF and the exchange interaction between excitons, which is given by (taking **p** and **q** as continuous variables for simplicity)

$$S_0[\psi^*(\mathbf{p}, t), \psi(\mathbf{p}, t)] = \mathcal{M}^2 \int \mathrm{d}t \int \mathrm{d}\mathbf{p}\,\mathrm{d}\mathbf{q} \times \left\{ \psi^*(\mathbf{p}, t) \left[\mathrm{i}\delta(\mathbf{p} - \mathbf{q}) \frac{\partial}{\partial t} + h(\mathbf{p}, \mathbf{q}) \right] \psi(\mathbf{q}, t) - V(\mathbf{p} - \mathbf{q}) \rho(\mathbf{p}, t) \rho(\mathbf{q}, t) \right\} \tag{27}$$

where $h(\mathbf{p}, \mathbf{q}) = E_{\mathbf{p}}\delta(\mathbf{p}-\mathbf{q}) - V(\mathbf{p}-\mathbf{q})[1-\rho(\mathbf{p}, t)]$, $\rho(\mathbf{p}, t) = \psi^*(\mathbf{p}, t)\psi(\mathbf{p}, t)$ is the quasi-boson occupancy in the **p** state, and $\delta(\mathbf{p} - \mathbf{q})$ is the Dirac delta function. $\mathcal{M}$ is a coefficient introduced for converting discrete **p** to a continuous variable. For a 2D system, $\mathcal{M} = s/4\pi^2$, where s is the area used to normalize exciton wavefunctions. From the expression of $h(\mathbf{p}, \mathbf{q})$, we find that the Coulomb interaction that correlates an electron and hole to form an exciton is reduced by a factor $1 - \rho(\mathbf{p}, t)$.

The action S_I is the interaction of the system with an optical pulse that is given by

$$S_I = -\mathcal{M} \int \mathrm{d}t\, [\mathcal{E}(t) \cdot \mathbf{M}_{cv}] \int \mathrm{d}\mathbf{p}\, \psi^*(\mathbf{p}, t)[1 - \rho(\mathbf{p}, t)]. \tag{28}$$

The interaction with a THz pulse is given by

$$S_T = -\mathcal{M}^2 \int \mathrm{d}t\, \mathbf{E}_{\mathrm{THz}}(t) \cdot \int \mathrm{d}\mathbf{p}\,\mathrm{d}\mathbf{q}\, \mathbf{K}(\mathbf{q}, \mathbf{p}) \psi^*(\mathbf{p}, t)\psi(\mathbf{q}, t) \times [1 - \rho(\mathbf{p}, t)], \tag{29}$$

which will be taken as a perturbation in the remainder of this paper. In constructing S_I and S_T, both the optical and the THz pulses are represented as classical fields. In other situations, a quantized optical field may be necessary and can be integrated into this method. The resulting effective action S ensures that the variation of the action $\delta S[\psi^*(\mathbf{p}, t), \psi(\mathbf{p}, t)]/\delta\psi^*(\mathbf{p}, t) = 0$ will reproduce the correct dynamic equation for $\psi(\mathbf{p}, t)$ and recovers equation (9). Here $\delta S/\delta\psi^*$ denotes the functional derivative with respect to ψ^*.

To proceed further, we apply the linear response theory to investigate intraexcitonic transitions induced by a THz pulse after the system is optically excited. With the THz pulse, the system is described by $\psi(\mathbf{p}, t)$, which differs from the mean field $\psi_0(\mathbf{p}, t)$ (the wavefunction describing the system after the optical excitation) by a small quantity $\zeta(\mathbf{p}, t)$. Following the procedure of the linear response theory [41], the equation for $\zeta(\mathbf{p}, t)$ is found to be

$$\int \mathrm{d}\mathbf{v}\left[\left(\mathrm{i}\frac{\partial}{\partial t}+E_{\mathbf{v}}\right)\delta(\mathbf{u}-\mathbf{v})-V(\mathbf{u}-\mathbf{v})\right]\zeta(\mathbf{v},t)$$
$$-2\int \mathrm{d}\mathbf{v}\,V(\mathbf{u}-\mathbf{v})[\psi_0(\mathbf{u},t)\psi_0^*(\mathbf{v},t)-\rho_0(\mathbf{u},t)]\zeta(\mathbf{v},t)$$
$$-2[F_0(\mathbf{u},t)-\psi_0^*(\mathbf{u},t)G_0(\mathbf{u},t)]\zeta(\mathbf{u},t)$$
$$+2\psi_0(\mathbf{u},t)\int \mathrm{d}\mathbf{v}\,V(\mathbf{u}-\mathbf{v})\psi_0(\mathbf{v},t)[\zeta^*(\mathbf{u},t)-\zeta^*(\mathbf{v},t)]$$
$$=E_{\mathrm{THz}}(t)\int \mathrm{d}\mathbf{v}\,K(\mathbf{u},\mathbf{v})\psi_0(\mathbf{v},t)[1-2\rho_0(\mathbf{u},t)], \tag{30}$$

where $F_0(\mathbf{u},t)=\int \mathrm{d}\mathbf{v}\,V(\mathbf{u}-\mathbf{v})\rho_0(\mathbf{v},t)$, $G_0(\mathbf{u},t)=\int \mathrm{d}\mathbf{v}\,V(\mathbf{u}-\mathbf{v})\psi_0(\mathbf{v},t)$, and $\rho_0(\mathbf{q},t)=|\psi_0(\mathbf{q},t)|^2$. In equation (30), we have neglected terms involving the optical pulses for simplicity, this amounts to assuming that there is no overlap between the optical pulse and the THz pulse.

The ground state $|\Psi_{\mathrm{MF}}\rangle$, which is determined by $\psi_0(\mathbf{p},t)$ can be obtained by solving the dynamic equation derived from the action S_0+S_{I} as we have done in previous publications using the density matrix method [21, 22]. For the experimental situation that we are considering (1s heavy-hole excitons are excited resonantly), it has been found experimentally [18] and numerically [21, 22] that 1s excitons dominate both the population and the photoluminescence. Thus a reasonable approximation to $\psi_0(\mathbf{p},t)$ is given by [39]

$$\psi_0(\mathbf{p},t)=\sqrt{N_{1\mathrm{s}}}\,c_{1\mathrm{s}}^{\mathbf{p}*}\exp[-\mathrm{i}\tilde{E}_{1\mathrm{s}}t-\mathrm{i}\gamma_{\mathbf{p}}], \tag{31}$$

where $N_{1\mathrm{s}}$ is the 1s excitons' population. The energy $\tilde{E}_{1\mathrm{s}}=E_{1\mathrm{s}}+\delta E_{1\mathrm{s}}$ is the density renormalized energy of the 1s exciton state. Here $\gamma_{\mathbf{p}}(t)$ describes the coherence status of the system. In equation (30), $\psi_0(\mathbf{p},t)$ acts as an important parameter, determining the dynamics of the system. In particular, as we will see, $\gamma_{\mathbf{p}}$ plays an important role in determining the resonance frequency of the 1s–2p intraexcitonic transition.

The initial value problem shown in equation (30) may be solved numerically provided that $\gamma_{\mathbf{p}}$ is treated properly. However, analytical results are more desirable to gain better understanding of the nature of intraexcitonic transitions, and will be pursued in the remainder of this section. The generation of 2p excitons can be quantified by projecting $\psi(\mathbf{p},t)$ onto the 2p state, which is given by

$$\Phi_{2\mathrm{p}}(t)=\sum_{\mathbf{q}}c_{2\mathrm{p}}^{\mathbf{q}}[\psi_0(\mathbf{q},t)+\zeta(\mathbf{q},t)], \tag{32}$$

and the contribution due to the THz pulse is $\sum_{\mathbf{q}}c_{2\mathrm{p}}^{\mathbf{q}}\zeta(\mathbf{q},t)$ (the other contribution is from the decoherence of the system). We will focus on this term and examine its time dependence. To this end, we introduce a general basis $\zeta_\mu(t)\equiv\sum_{\mathbf{p}}c_\mu^{\mathbf{p}}\zeta(\mathbf{p},t)$. Using the orthogonality of $c_\mu^{\mathbf{p}}$, we obtain $\zeta(\mathbf{p},t)=\sum_\mu c_\mu^{\mathbf{p}*}\zeta_\mu(t)$ and find equation (30) can be written as

$$\mathrm{i}\frac{\mathrm{d}}{\mathrm{d}t}\zeta_{2\mathrm{p}}(t)=-E_{2\mathrm{p}}\zeta_{2\mathrm{p}}(t)+\sum_\mu(U_\mu+W_\mu)\zeta_\mu(t)$$
$$+2\sum_\mu D_\mu(t)\zeta_\mu^*(t)+E_{\mathrm{THz}}(t)K_{1\mathrm{s}-2\mathrm{p}}, \tag{33}$$

where $E_{2\mathrm{p}}$ is the energy of a single 2p exciton. We also have

$$U_\mu=2N_{1\mathrm{s}}\mathcal{M}^2\int \mathrm{d}\mathbf{u}\,\mathrm{d}\mathbf{v}\,V(\mathbf{u}-\mathbf{v})c_{2\mathrm{p}}^{\mathbf{u}}(|c_{1\mathrm{s}}^{\mathbf{v}}|^2c_\mu^{\mathbf{u}*}$$
$$-|c_{1\mathrm{s}}^{\mathbf{u}}|^2c_\mu^{\mathbf{v}*}), \tag{34}$$

$$W_\mu=2N_{1\mathrm{s}}\mathcal{M}^2\int \mathrm{d}\mathbf{u}\,\mathrm{d}\mathbf{v}\,V(\mathbf{u}-\mathbf{v})c_{2\mathrm{p}}^{\mathbf{u}}[c_{1\mathrm{s}}^{\mathbf{u}}c_{1\mathrm{s}}^{\mathbf{v}*}c_\mu^{\mathbf{v}*}\mathrm{e}^{\mathrm{i}(\gamma_{\mathbf{v}}-\gamma_{\mathbf{u}})}$$
$$-c_{1\mathrm{s}}^{\mathbf{u}*}c_{1\mathrm{s}}^{\mathbf{v}}c_\mu^{\mathbf{u}*}\mathrm{e}^{\mathrm{i}(\gamma_{\mathbf{u}}-\gamma_{\mathbf{v}})}], \tag{35}$$

and

$$K_{1\mathrm{s}-2\mathrm{p}}=\sqrt{N_{1\mathrm{s}}}\,\mathrm{e}^{-\mathrm{i}\tilde{E}_{1\mathrm{s}}t}$$
$$\times\mathcal{M}^2\int \mathrm{d}\mathbf{u}\,\mathrm{d}\mathbf{v}\,c_{2\mathrm{p}}^{\mathbf{u}*}K_{\mathbf{u},\mathbf{v}}[1-\rho(\mathbf{v},t)]c_{1\mathrm{s}}^{\mathbf{v}}\exp[-\mathrm{i}\gamma_{\mathbf{v}}(t)]. \tag{36}$$

We note that

$$D_\mu=N_{1\mathrm{s}}\mathcal{M}^2\mathrm{e}^{-\mathrm{i}2\tilde{E}_{1\mathrm{s}}t}\int \mathrm{d}\mathbf{u}\,\mathrm{d}\mathbf{v}\,c_{2\mathrm{p}}^{\mathbf{u}}c_{1\mathrm{s}}^{\mathbf{u}}c_{1\mathrm{s}}^{\mathbf{v}}V(\mathbf{u}-\mathbf{v})$$
$$\times(c_\mu^{\mathbf{u}}-c_\mu^{\mathbf{v}}) \tag{37}$$

is highly time dependent.

The fact that the expression of W_μ involves $\gamma_{\mathbf{p}}$ (U_μ contains no $\gamma_{\mathbf{p}}$) has an immediate implication: if $\gamma_{\mathbf{p}}$ has random values at different $\mathbf{p}$ points, $W_\mu\approx 0$[2], and can thus be ignored to a large extent; in contrast, if $\gamma_{\mathbf{p}}$ is a constant function of $\mathbf{p}$, then W_μ needs to be evaluated. This requires us to know the coherence status of the system under consideration.

From equations (33) and (36), we see that the resonance frequency of $\zeta_{2\mathrm{p}}$ is given by

$$\hbar\omega_{1\mathrm{s}-2\mathrm{p}}=E_{2\mathrm{p}}-\tilde{E}_{1\mathrm{s}}-U_{2\mathrm{p}}-W_{2\mathrm{p}}, \tag{38}$$

where $U_{2\mathrm{p}}$ and $W_{2\mathrm{p}}$ is the density-dependent correction to the resonance energy. Interestingly, we find that

$$U_{2\mathrm{p}}=2N_{1\mathrm{s}}\mathcal{M}^2\int \mathrm{d}\mathbf{u}\,\mathrm{d}\mathbf{v}\,V(\mathbf{u}-\mathbf{v})c_{2\mathrm{p}}^{\mathbf{u}}(|c_{1\mathrm{s}}^{\mathbf{v}}|^2c_{2\mathrm{p}}^{\mathbf{u}*}-|c_{1\mathrm{s}}^{\mathbf{u}}|^2c_{2\mathrm{p}}^{\mathbf{v}*})$$
$$=2N_{1\mathrm{s}}R_{2\mathrm{p},1\mathrm{s},1\mathrm{s}}^{2\mathrm{p}}, \tag{39}$$

which is closely related to $\delta E_{2\mathrm{p}}$ (compare with equation (20)). However, $W_{2\mathrm{p}}$ has no counterpart in section 3.1, thus equation (38) generalizes the simple expression shown in equation (23) by including effects caused by many-body interactions in the intraexcitonic transition process.

With the above results, we can now directly examine the resonance frequency of the 1s–2p intraexcitonic transition. We continue to use an ideal quantum well, which is a strict 2D system, as an example to work out the numerical values of $\hbar\omega_{1\mathrm{s}-2\mathrm{p}}$. The energy renormalization of 1s excitons had been obtained in equation (19), i.e. $\tilde{E}_{1\mathrm{s}}\simeq E_{1\mathrm{s}}+24.2E_{1\mathrm{s}}a_{2\mathrm{D}}^2n_{1\mathrm{s}}$, and $U_{2\mathrm{p}}\simeq 76.0E_{\mathrm{b}}a_{2\mathrm{D}}^2n_{1\mathrm{s}}$ is obtained using equations (39) and (20). We thus only need to compute $W_{2\mathrm{p}}$ to find $\hbar\omega_{1\mathrm{s}-2\mathrm{p}}$, for which we consider two extreme situations: the totally

[2] This conclusion is obtained with the assumptions that $V(\mathbf{u})$ and $c_\mu^{\mathbf{u}}$ ($\mu=$ 1s, 2p) are smooth functions of $\mathbf{u}$, and that $\gamma_{\mathbf{u}}$ varies rapidly with $\mathbf{u}$.

coherent case ($\gamma_{\mathbf{p}}$ is a constant), and the random phase case in which W_{2p} can be omitted.

In the first case, we find

$$W_{2p} = -138.4E_{1s}a_{2D}^2 n_{1s}, \tag{40}$$

implying that

$$\hbar\omega_{1s-2p} = (E_{2p} - E_{1s}) + 38.2a_{2D}^2 n_{1s}E_{1s},$$

which shows that the 1s–2p resonance frequency increases (blue-shifted) with the 1s exciton density. We note that $\delta(\hbar\omega_{1s-2p})/\delta E_{1s} \simeq 1.58$ in this case. On the other hand, in the second case we have

$$\hbar\omega_{1s-2p} = (E_{2p} - E_{1s}) - 100.2a_{2D}^2 n_{1s}E_{1s}, \tag{41}$$

implying that the energy difference between 2p and 1s exciton states decreases (red-shifted) as the 1s exciton density increases, and that

$$\delta(\hbar\omega_{1s-2p})/\delta E_{1s} \simeq -4.12, \tag{42}$$

which explains the experimental observation that shows $\hbar\omega_{1s-2p}$ decreases as exciton density increases, and that $\delta(\hbar\omega_{1s-2p})/\delta E_{1s} \simeq -4.0$ (estimated using the plot in [7]), strongly suggesting that in experiments the system has random phases at different $\mathbf{k}$ points.

We finally comment on the validity of adopting the random phase model in deriving equation (41). In experiments performed so far, exciton densities are well above 10^{10} cm^{-2} because of the limitation in the sensitivity of THz measurement techniques [15]. In the high exciton density regime, the scattering between different $\psi_{\mathbf{p}}$, which can destroy the phase coherence in the system, is hard to avoid. In addition, the several picoseconds time delay before the THz pulse interacts with excitons that were optically excited [7] will result in the loss of coherence between $\psi_{\mathbf{k}}$ at different $\mathbf{k}$ sites, while having a limited effect on the exciton population. Finally, unbound carriers can significantly alter the phase of $\psi_{\mathbf{p}}$ at different $\mathbf{p}$ points. Therefore we believe it is reasonable to use the random phase model in this study.

3.3. Discussion of the excitonic approach

In our investigation, the bandgap E_g is assumed to be a constant. It has been shown [42] that, due to the electron–electron and electron–phonon interactions, a renormalization can happen to E_g at high carrier densities (typically, the carrier density n is well beyond 10^{11} cm^{-2} when this renormalization is considered) or high temperatures when the phonon population becomes large [43–45]. We did not need to consider the bandgap renormalization for three reasons. First, the carrier densities we considered are below $n = 10^{11}$ cm^{-2} when exciton signatures are still strong, in which no bandgap renormalizations were reported. Second, given a certain exciton density, E_g has the same value for 1s, 2p... excitonic states. Thus the energy difference between two excitonic states (e.g. equation (41)), which is the central result of this work, should be independent of E_g, whether it is renormalized or not. Furthermore, the universality of bandgap renormalization [43–45] (the measured dependence of E_g only slightly depends on material or the width of a quantum well) strongly hints that the renormalization is in fact associated with the energy levels of carriers, which is the perspective some authors had adopted: finding how the energy levels of a carrier, not the bandgap, are affected by many-body interactions [19].

The excitonic approach presented in this paper has its strengths and weaknesses. Using this approach, the THz-pulse-induced carrier dynamics can be intuitively understood as transitions between internal exciton states, and numerical and analytical results can be derived to estimate how the transitions are affected by other factors such as exciton densities. The excitonic approach's limitations are mainly due to the many-body interactions it can handle, at the same time keeping the approach tractable.

One limitation is how many exciton states we include in our calculations. As 1s exciton density increases, many-body interactions redistribute carriers dynamically to accommodate new excitons (compare with equation (10)), creating excitons with higher internal states (2s, 2p, ...) and nonzero COM motions. To fully describe carrier dynamics, a complete excitonic basis, which combines both the internal states and COM motions of an exciton, are desirable. However, an excitonic approach involving too many basis states will cause difficulty in numerical calculation, losing its advantages [22]. It is thus necessary, when applying the excitonic approach, to restrict ourselves to investigating low to medium exciton densities ($<10^{11}$ cm^{-2}), for which a large portion of excitons remains in the $\mathbf{K} = 0$, 1s state [22, 28] when 1s excitons are resonantly created. For higher carrier densities, equations obtained using the dynamics controlled truncation method [46] may be a better choice. We note, however, that the restriction to $\mathbf{K} = 0$ quasi-bosons, a practice employed in this paper, is not a new type of approximation. In fact, a careful comparison [21] was carried out to demonstrate that, with further simplifications, the dynamic equations for $\langle B_{\mathbf{p}}^{\dagger}\rangle$ and $\langle B_{\mathbf{p}}^{\dagger}B_{\mathbf{q}}\rangle$ (compare with equation (9)) can be reduced to the Hartree–Fock order semiconductor Bloch equations (SBEs) [33]. Thus, the approximation we used is similar to that used in deriving SBEs. Another complication is from a plasma of unbound but correlated electrons and holes created by a nonresonant excitation condition or high lattice temperatures [15]. This problem can be partially remedied by tuning the mean field in equation (31) to mimic this situation, but in general the dielectric THz responses of unbound carriers may need a separate treatment [15]. In principle, the excitonic approach can include effects due to free carriers by including more bound and unbound excitonic states, but this will cause analytical and computational difficulties, thus invalidating the reasons for choosing an excitonic approach.

We finally note that other processes, such as the formation of biexcitons [54, 55] and Auger recombination [56, 57], can further complicate the analysis on the intraexcitonic transitions at high exciton concentrations. If biexcitonic effects are of interest, we could derive equations for $\langle B_{\mathbf{p}}^{\dagger}B_{\mathbf{q}}^{\dagger}\rangle$ and perform factorizations to retain terms related to biexcitons [28, 52, 53]. For the exciton density ($\lesssim 10^{11}$ cm^{-2})

we are interested in, the inter-particle distance $r_s \simeq 3.6$,[3] which implies the average distance between excitons is much larger than their radius and biexciton formation can be largely neglected. The Auger recombination process, which usually involves more than three particles, is normally only significant in non-equilibrium conditions when the exciton density is very high [58]. As a scattering process, Auger recombinations can potentially have several effects: (1) reduce exciton lifetime; (2) increase the number of free electrons/holes; (3) cause loss of coherence between $\psi_{\mathbf{k}}$ at different $\mathbf{k}$ sites. However, using the Auger recombination rate obtained in [57, 58], it can be shown that this process only has minimal effect on exciton lifetime, as well as other effects, at the density of $\lesssim 10^{11}$ cm^{-2}.

4. Conclusion

In this work, we investigated intraexcitonic dynamics induced by a THz pulse in an optically excited exciton system. We have theoretically shown that the 1s–2p exciton resonance frequency is red-shifted as exciton densities increase. In [15], the THz dielectric responses due to both excitons and unbound electron–hole pairs are computed using Fermi's golden rule and the Drude model. From our results, we believe the phase coherence (described by $\gamma_{\mathbf{p}}$) of the system, which is largely determined by many-body interactions, is another important factor that accounts for the dynamics of intraexcitonic transitions. While the exciton system considered in this study has random phases, there are other systems that might have perfect phase coherence, notably an excitonic condensate [47, 48], in which the THz induced intraexcitonic transitions can have different properties, e.g. showing blue-shift instead of red-shift as exciton density increases.

The mean-field method presented in this study, including the effective action and the derivation of equation (30), can be applied to more general problems related to exciton systems. For example, using a quantized optical field in the effective action in equations (28) and (29), our mean-field method can be extended to the study of excitons in microcavities or photonic crystals, in which strong interactions between excitons and photons result in exciton–polaritons [49–51]. We hope our model and approach can serve as a useful tool for the investigation of exciton dynamics in these systems in the future.

Acknowledgments

We thank Professor Marc M Dignam for many insightful discussions. This work is supported by the National Natural Science Foundation of China under grant No. 10904122 and the Ministry of Education of China.

References

[1] Timusk T 1976 *Phys. Rev.* B **13** 3511
[2] Groeneveld R H M and Grischkowsky D 1994 *J. Opt. Soc. Am.* B **11** 2502
[3] Černe J, Kono J, Sherwin M S, Sundaram M, Gossard A C and Bauer G E W 1996 *Phys. Rev. Lett.* **77** 1131
[4] Salib M S, Nickel H A, Herold G S, Petrou A, McCombe B D, Chen R, Bajaj K K and Schaff W 1996 *Phys. Rev. Lett.* **77** 1135
[5] Johnsen K and Kavoulakis G M 2001 *Phys. Rev. Lett.* **86** 858
[6] Kaindl R A, Carnahan M A, Hagele D, Lovenich R and Chemla D S 2003 *Nature* **423** 734
[7] Huber R, Kaindl R A, Schmid B A and Chemla D S 2005 *Phys. Rev.* B **72** 161314
[8] Lloyd-Hughes J, Beere H E, Ritchie D A and Johnston M B 2008 *Phys. Rev.* B **77** 125322
[9] Jörger M, Fleck T, Klingshirn C and von Baltz R 2005 *Phys. Rev.* B **71** 235210
[10] Karpinska K, van Loosdrecht P H M, Handayani I P and Revcolevschi A 2005 *J. Lumin.* **112** 17
[11] Kubouchi M, Yoshioka K, Shimano R, Mysyrowicz A and Kuwata-Gonokami M 2005 *Phys. Rev. Lett.* **94** 016403
[12] Huber R, Schmid B A, Shen Y R, Chemla D S and Kaindl R A 2006 *Phys. Rev. Lett.* **96** 017402
[13] Tayagaki T, Mysyrowicz A and Kuwata-Gonokami M 2006 *Phys. Rev.* B **74** 245127
[14] Galbraith I *et al* 2005 *Phys. Rev.* B **71** 073302
[15] Kaindl R A, Hägele D, Carnahan M A and Chemla D S 2009 *Phys. Rev.* B **79** 045320
[16] Grunwald T, Jung T, Kohler D, Koch S, Khitrova G, Gibbs H, Hey R and Chatterjee S 2009 *Phys. Status Solidi* c **6** 500
[17] Kaindl R A, Huber R, Schmid B A, Carnahan M A, Hagele D and Chemla D S 2006 *Phys. Status Solidi* b **243** 2414
[18] Peyghambarian N, Gibbs H M, Jewell J L, Antonetti A, Migus A, Hulin D and Mysyrowicz A 1984 *Phys. Rev. Lett.* **53** 2433
[19] Schmitt-Rink S, Chemla D S and Miller D A B 1985 *Phys. Rev.* B **32** 6601
[20] Hulin D, Mysyrowicz A, Antonetti A, Migus A, Masselink W T, Morkoç H, Gibbs H M and Peyghambarian N 1986 *Phys. Rev.* B **33** 4389
[21] Wang D, Hawton M and Dignam M M 2007 *Phys. Rev.* B **76** 115311
[22] Wang D and Dignam M M 2009 *Phys. Rev.* B **79** 165320
[23] Kira M, Hoyer W, Stroucken T and Koch S W 2001 *Phys. Rev. Lett.* **87** 176401
[24] Dignam M and Hawton M 2003 *Phys. Rev.* B **67** 035329
[25] Combescot M and Betbeder-Matibet O 2003 *Europhys. Lett.* **62** 140
[26] Combescot M and Betbeder-Matibet O 2010 *Phys. Rev. Lett.* **104** 206404
[27] Yang L, Rosam B, Lachaine J-M, Leo K and Dignam M M 2004 *Phys. Rev.* B **69** 165310
[28] Yang Z S, Kwong N H, Takayama R and Binder R 2005 *Europhys. Lett.* **69** 417
[29] Hawton M and Nelson D 1998 *Phys. Rev.* B **57** 4000
[30] Chernyak V, Zhang W M and Mukamel S 1998 *J. Chem. Phys.* **109** 9587
[31] Usui T 1960 *Prog. Theor. Phys.* **23** 787
[32] Wang D 2008 An excitonic approach to the ultrafast optical response of semiconductor nano-structures *PhD Thesis* Queen's University at Kingston
[33] Haug H and Koch S 1990 *Quantum Theory of the Optical and Electronic Properties of Semiconductors* (Singapore: World Scientific)
[34] Andreani L C and Pasquarello A 1990 *Phys. Rev.* B **42** 8928
[35] Mathieu H, Lefebvre P and Christol P 1992 *Phys. Rev.* B **46** 4092
[36] Dignam M M and Sipe J E 1990 *Phys. Rev.* B **41** 2865
[37] Choi M, Je K -C, Yim S-Y and Park S-H 2004 *Phys. Rev.* B **70** 085309
[38] Zhu X, Littlewood P B, Hybertsen M S and Rice T M 1995 *Phys. Rev. Lett.* **74** 1633
[39] Imamog lu A, Ram R J, Pau S and Yamamoto Y 1996 *Phys. Rev.* A **53** 4250

[3] We assume the exciton density $n = 10^{11}$ cm^{-2} and the radius of a 1s exciton is 50 Å.

[40] Littlewood P B, Eastham P R, Keeling J M J, Marchetti F M, Simons B D and Szymanska M H 2004 *J. Phys.: Condens. Matter* **16** S3597
[41] DeWitt B 2003 *The Global Approach to Quantum Field Theory* (*The International Series of Monographs on Physics* vol 114) (Oxford: Oxford University Press)
[42] Das Sarma S, Jalabert R and Yang S-R E 1990 *Phys. Rev.* B **41** 8288
[43] Tränkle G, Lach E, Forchel A, Scholz F, Ell C, Haug H, Weimann G, Griffiths G, Kroemer H and Subbanna S 1987 *Phys. Rev.* B **36** 6712
[44] Tränkle G, Leier H, Forchel A, Haug H, Ell C and Weimann G 1987 *Phys. Rev. Lett.* **58** 419
[45] Das Sarma S, Jalabert R and Yang S-R E 1989 *Phys. Rev.* B **39** 5516
[46] Axt V M and Stahl A 1994 *Z. Phys.* B **93** 195
[47] Lozovik Y E and Yudson V I 1976 *Sov. Phys.—JETP* **44** 389
[48] Hammack A T, Griswold M, Butov L V, Smallwood L E, Ivanov A L and Gossard A C 2006 *Phys. Rev. Lett.* **96** 227402
[49] Utsunomiya S *et al* 2008 *Nature Phys.* **4** 700
[50] Goldberg D, Deych L I, Lisyansky A A, Shi Z, Menon V M, Tokranov V, Yakimov M and Oktyabrsky S 2009 *Nature Photon.* **3** 662
[51] Amo A *et al* 2009 *Nature* **457** 291
[52] Rumyantsev I, Kwong N H, Binder R, Gansen E J and Smirl A L 2004 *Phys. Rev.* B **69** 235329
[53] Kner P, Bar-Ad S, Marquezini M V, Chemla D S, Lövenich R and Schäfer W 1999 *Phys. Rev.* B **60** 4731
[54] Klimov V, Hunsche S and Kurz H 1994 *Phys. Rev.* B **50** 8110
[55] Takayama R, Kwong N, Rumyantsev I, Kuwata-Gonokami M and Binder R 2002 *Eur. Phys. J.* B **25** 445
[56] Dutta N K 1983 *J. Appl. Phys.* **54** 1236
[57] Hausser S, Fuchs G, Hangleiter A, Streubel K and Tsang W T 1990 *Appl. Phys. Lett* **56** 913
[58] Shen Y C, Mueller G O, Watanabe S, Gardner N F, Munkholm A and Krames M R 2007 *Appl. Phys. Lett.* **91** 141101